

## Development, And Characterization Of Ligand-Conjugated Gemcitabine Multiwalled Carbon Nanotubes For The Treatment Of Lung Cancer

Pushpendra Kumar Khangar<sup>1\*</sup>, Vivek Daniel<sup>2</sup>

<sup>1</sup>Research Scholar, Oriental University, Indore, Opp. Reoti Range, Gate No.1, Jakhya, Sanwer Road, Indore, 453555, India.

<sup>2</sup> Professor, Oriental University, Indore, Faculty of Pharmacy, [Opp. Reoti Range, Gate No.1, Jakhya, Sanwer Road, Indore, 453555, India.](#)

---

Cite this paper as: Pushpendra Kumar Khangar, Vivek Daniel (2024). Development, And Characterization Of Ligand-Conjugated Gemcitabine Multiwalled Carbon Nanotubes For The Treatment Of Lung Cancer. *Frontiers in Health Informatics*, 13 (8) 3057-3070

---

### ABSTRACT:

Lung cancer is the most frequently diagnosed cancer globally, with an estimated 2.2 million new cases in 2020. It is a major cause of cancer-related mortality, accounting for roughly 1.8 million deaths each year. The disease is categorized into two main types: non-small cell lung cancer (NSCLC), which is more common and typically develops at a slower rate, and small cell lung cancer (SCLC), which is less common but grows and spreads more quickly.

The leading risk factor for lung cancer is smoking, which is responsible for approximately 85% of all cases. Passive smoking, or exposure to second-hand smoke, is also a well-established risk factor. Additionally, air pollution, particularly fine particulate matter (PM<sub>2.5</sub>), significantly increases lung cancer risk. Exposure to hazardous substances, such as asbestos and radon, further increases the likelihood of developing the disease. Occupational exposure to carcinogens contributes to an estimated 9–15% of lung cancer cases. Research also highlights a potential link between lung cancer and viruses, such as human papillomaviruses (HPV).

The primary prevention strategy for lung cancer is tobacco control and smoking prevention. Lung cancer screening with low-dose computed tomography (LDCT) can reduce mortality by detecting cancer early. Approximately 90% of lung cancer patients initially present with non-specific symptoms, such as cough, weight loss, chest pain, and dyspnea, often causing diagnostic delays.

Basic diagnostic procedures include medical history and clinical examination, Laboratory tests (blood count, liver and kidney function, coagulation, electrolytes), Chest X-ray (initial imaging), Spiral CT of the thorax (contrast-enhanced), Bronchoscopy, Abdominal ultrasound

Treatment depends on the cancer type and stage, involving surgery, radiation, chemotherapy, targeted therapy, and immunotherapy. Early-stage NSCLC with complete tumor resection has improved 5-year survival rates, with up to 72% survival in stage IA. However, 60–70% of SCLC cases are diagnosed at advanced stage IV, with a 5% two-year survival rate.

Carbon nanotubes (CNTs) offer a cutting-edge approach to lung cancer treatment by enabling precise drug delivery, reducing side effects, and targeting cancer cells while sparing healthy tissue. Their nanoscale size ensures deep tumor

penetration, while their multifunctional capabilities support combination therapies and photothermal treatments. CNTs also overcome drug resistance, facilitate real-time monitoring, and enable early intervention, making them a promising tool for improving outcomes and quality of life in lung cancer patients.

This study aimed to target lung cancer cells, to reduce the overall toxicity of the cytotoxic drugs.

**KEYWORDS:** Lung cancer, MWCNTs, Apoptosis, Chemotherapy, Carcinoma

## INTRODUCTION :

### Background

Lung cancer remains one of the most prevalent and fatal cancers globally, necessitating innovative treatment strategies to enhance therapeutic efficacy while minimizing harm to normal tissues<sup>(1)</sup>. Targeting cancer cells using nanotechnology has gained significant attention<sup>(2)</sup>, particularly the use of multi-walled carbon nanotubes (MWCNTs) due to their unique properties such as high surface area, thermal conductivity, and capacity for functionalization<sup>(3)</sup>.

One promising approach involves functionalizing MWCNTs with folic acid (FA) ligands<sup>(4)</sup>. Folic acid is a well-known targeting agent because many cancer cells, including lung cancer cells, overexpress folate receptors on their surface<sup>(5)</sup>. By conjugating MWCNTs with folic acid, these nanocarriers can selectively bind to and enter cancer cells through receptor-mediated endocytosis, leaving normal cells largely unaffected<sup>(6)</sup>. This targeted delivery significantly reduces systemic toxicity associated with traditional chemotherapeutic agents<sup>(7)</sup>.

Moreover, MWCNTs can be loaded with therapeutic agents, such as chemotherapeutic drugs, and release them in a controlled manner at the tumor site, further enhancing treatment efficacy<sup>(8)</sup>. The combination of folic acid targeting and MWCNT-based delivery offers a dual advantage of improving drug bioavailability at the tumor site and minimizing off-target effects<sup>(9)</sup>. This approach not only enhances the therapeutic index of cancer treatments but also reduces side effects, improving the overall quality of life for patients.

This innovative strategy represents a significant step forward in precision medicine, leveraging both the specificity of folic acid targeting and the versatility of MWCNTs to advance lung cancer treatment.

### Significance

Targeting lung cancer cells using folic acid-functionalized multiwalled carbon nanotubes (MWCNTs) represents a significant advancement in cancer therapy by addressing critical challenges like systemic toxicity and poor specificity<sup>(10)</sup>. Folic acid ligands ensure precise targeting by binding to overexpressed folate receptors on lung cancer cells, allowing selective delivery of therapeutic agents<sup>(11)</sup>. This reduces damage to healthy tissues and minimizes side effects<sup>(12)</sup>. Additionally, MWCNTs offer high drug-loading capacity and controlled release, enhancing therapeutic efficacy while reducing drug resistance<sup>(13)</sup>. Their multifunctionality enables the integration of imaging and treatment, aligning with the principles of precision medicine<sup>(14)</sup>. This innovative approach improves patient outcomes by increasing treatment success, extending survival, and enhancing quality of life, marking a major step forward in personalized lung cancer care<sup>(15)</sup>.

## MATERIAL AND METHODS/ METHODOLOGY

Research-grade multi-walled carbon nanotubes (MWCNTs), prepared using the chemical vapor deposition (CVD) method, were sourced from Shilpent (Shilpa Enterprises). The MWCNTs had a purity of 99% and a CNT content of 95–99%. Their dimensions were specified as an outer diameter of 5–30 nm and a length of 10–30 micrometers, with a bulk density of 0.04 g/cm<sup>3</sup>. A 10 g pack was used for the study. The Gemcitabine was purchased from B L Chemicals. EDC

(1-ethyl-3-(3-dimethyl aminopropyl) carbodiimide) obtained from Sigma Aldrich, and NHS (N-hydroxysuccinimide) and folic acid obtained from Sigma Aldrich were used in this study. All the ingredients were of Analytical grade.

### FUNCTIONALIZATION OF MWCNTs

To improve the solubility and provide sites for conjugation, MWCNTs were functionalized:

The following procedure was undertaken to conjugate Gemcitabine to multi-walled carbon nanotubes (MWCNTs):

Multi-walled carbon nanotubes (MWCNTs) (100 mg) were treated with a mixture of concentrated nitric acid ( $\text{HNO}_3$ , 5 mL) and sulfuric acid ( $\text{H}_2\text{SO}_4$ , 15 mL) in a 1:3 volume ratio. The reaction mixture was sonicated for 3 hours at 80 °C-100 °C to introduce carboxylic (-COOH) groups onto the MWCNTs. Afterward, the mixture was neutralized by washing thoroughly with deionized water until a neutral pH was achieved. The oxidized MWCNTs were then dried under a vacuum at 60 °C.

The oxidized MWCNTs (50 mg) were dispersed in 10 mL of MES buffer (0.1 M, pH 6.0) by sonication. EDC (N-(3-Dimethylaminopropyl)-N'-ethylcarbodiimide, 40 mg) and NHS (N-Hydroxysuccinimide, 25 mg) were added to activate the carboxylic groups, forming reactive ester intermediates. The solution was stirred for 1 hour at room temperature. There may be two possibilities MWCNT-(COO-NHS)<sub>n</sub>, Which shows complete esterification, and (MWCNT)-[C(O)-OH]<sub>x</sub>-[C(O)-ONHS]<sub>y</sub> which represents some residual -COOH groups.

Folic acid (30 mg) was dissolved in 10 mL of the same MES buffer and added to the activated MWCNTs. The reaction mixture was stirred at 30 °C for 12 hours to allow the formation of stable amide bonds. The MWCNT-FA conjugates were washed with deionized water several times to remove unreacted folic acid and dried under a vacuum.

The final conjugate can be represented as MWCNT-[CO-NH-Folic Acid]<sub>n</sub>

MWCNT-FA conjugates (30 mg) were dispersed in 10 mL of phosphate-buffered saline (PBS, pH 7.4). Gemcitabine (10 mg) was added to the dispersion, and the mixture was stirred gently at 4 °C for 24 hours to maximize drug loading. The mixture was dialyzed against PBS using a dialysis membrane (molecular weight 10 kDa) for 12 hours to remove the unbound drug.

Dialysis and ultrafiltration were performed to remove free molecules, such as unreacted folic acid and unbound Gemcitabine. The product was washed thoroughly with deionized water and collected as a purified dispersion.

The purified dispersion was frozen at -80 °C and freeze-dried to obtain a stable powder form of the MWCNT-FA-Gemcitabine conjugate, ensuring long-term stability and ease of handling.

### Characterization of Gemcitabine loaded MWCNTs

#### a) Characterization of Drug Conjugation to MWCNT

IR spectroscopy was conducted according to standard procedures. The Bruker Alpha model, Germany (ATR technique). IR spectra of pure and functionalized MWCNT were noted from 4,000 to 400  $\text{cm}^{-1}$ . The spectra confirm the chemical bonding of the Gemcitabine to MWCNTs and functionalization, etc.

#### b) Entrapment efficiency

The amount of drug entrapped in the formulations was calculated by estimating the amount of un-entrapped drug by dissolving 10 mg powder in phosphate buffer pH 7.4. The obtained solution was assayed spectrophotometrically at 268

nm for free drug content.

The % entrapment efficiency was determined spectrophotometrically (UV/Vis 1600, Shimadzu, Japan) at 268 nm (characteristic absorbance of GEM) using the following formula:

% Entrapment Efficiency = Weight of entrapped GEM in formulation/Weight of entrapped GEM + free GEM X 100

#### **c) Drug content**

The drug content of the Gemcitabine-loaded MWCNT was analysed by dissolving the formulation in an appropriate amount of phosphate buffer (pH 7.4) with the assistance of an ultra-sonicator. The drug content was measured at a wavelength of 268 nm using a Shimadzu 1600 spectrophotometer (Japan).

#### **d) Particle size determination**

##### **The Dynamic Light Scattering (DLS)**

The Dynamic Light Scattering (DLS) method is a widely used technique for determining the average particle size in a sample <sup>(16)</sup>. It measures the fluctuations in the intensity of scattered light caused by the Brownian motion of particles in a suspension. By analyzing these fluctuations, the hydrodynamic diameter of the particles can be calculated, providing information about the particle size distribution <sup>(17)</sup>.

DLS (Dynamic Light Scattering) which represented the average size of multi-walled carbon nanotubes (MWCNTs). The mean size was found to be 70 nm, while the Gaussian-like curve illustrates the relative intensity versus particle size.

#### **e) Mass spectroscopy**

Mass spectrometry (MS) is a powerful analytical technique used to identify and quantify molecules based on their mass-to-charge ratio ( $m/z$ ) <sup>(18)</sup>. It has a wide range of applications across various fields, including Chemical Identification determining the molecular structure and composition of organic and inorganic compounds <sup>(19)</sup>.

#### **f). Zeta potential**

Zeta potential is a measure of the electrical potential at the interface between a particle and its surrounding liquid, playing a key role in the stability of colloidal systems<sup>(20)</sup>. High zeta potential values indicate strong electrostatic repulsion between particles, preventing aggregation and ensuring stability, while low values can lead to particle clumping <sup>(21)</sup>. It is widely used in applications such as drug delivery, where it helps assess the stability and behaviour of nanoparticles, as well as in industries like cosmetics, food, and wastewater treatment. Zeta potential is typically measured using electrophoretic light scattering and is crucial for optimizing formulations and processes in various fields <sup>(22)</sup>.

#### **g). X-Ray Diffraction XRD**

X-Ray Diffraction (XRD) is an analytical technique used to study the structure, composition, and physical properties of materials at the atomic or molecular level<sup>(23)</sup>. It is based on the diffraction of X-rays when they interact with the regular arrangement of atoms in a crystalline material<sup>(24)</sup>. XRD of Pristine MWCNTs and drug-loaded MWCNTs was performed.

#### **h) Raman Spectroscopy**

Raman spectroscopy is a powerful, non-destructive analytical technique that provides valuable insights into molecular structure, composition, and interactions<sup>(25)</sup>. It identifies functional groups and molecular bonds by analyzing vibrational modes and distinguishes between chemical compounds through unique vibrational fingerprints<sup>(26)</sup>. Raman spectrum of Pristine Vs Folic acid conjugated MWCNTs, Folic acid conjugated MWCNTs and MWCNTs-FA/ Gemcitabine was determined.

### **RESULT AND DISCUSSION:**

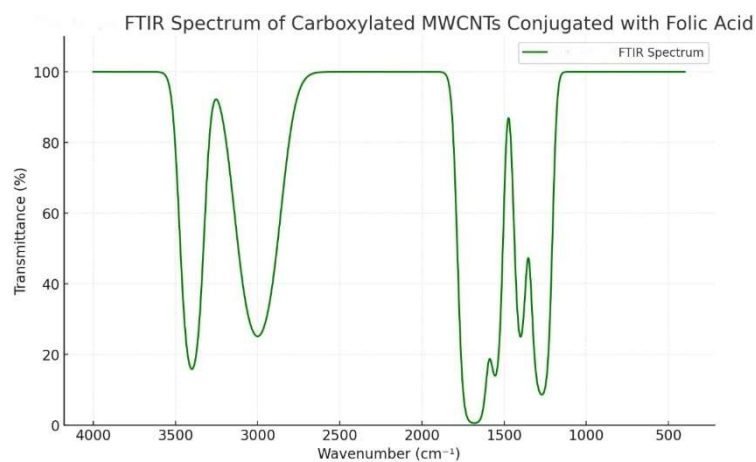
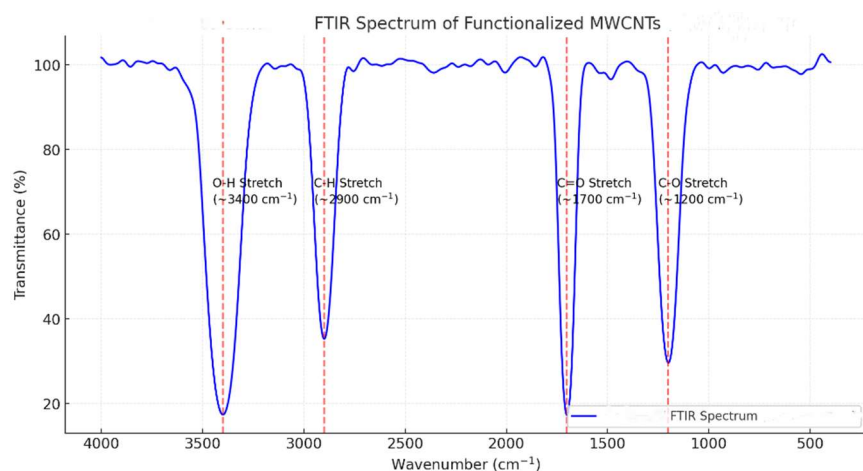
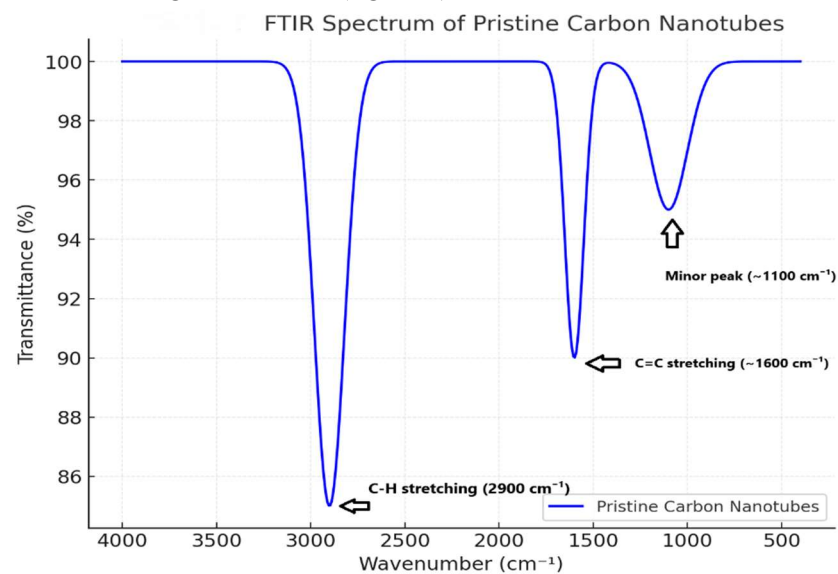
#### **Functionalization of CNTs and drug loading**

The MWCNTs were acid treated for functionalization (-COOH) group was confirmed by FTIR, after which FA was attached as ligand and then the drug was loaded using non-covalent bonding.

#### **IR spectroscopy**

The pure MWCNT has no obvious characteristic absorption peaks. The spectra of MWCNT indicated intensive bands at

ideal wavelengths shown in (figure 1).



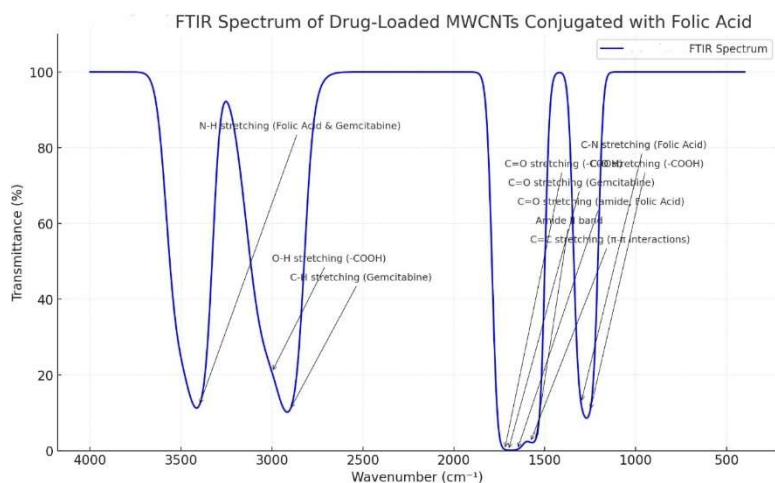


**Figure 1. IR spectroscopy of (A) pristine MWCNT & (B) functionalized MWCNT-COOH (C) MWCNTs-FA (D) MWCNTs-FA/Gemcitabine**

### Observed FTIR Regions

**Broad O-H/N-H Stretching:**  $\sim 3200\text{-}3600\text{ cm}^{-1}$  (indicates hydrogen bonding and the presence of hydroxyl and amine groups).

**C=O Stretching:**  $\sim 1650\text{-}1750\text{ cm}^{-1}$  (indicates carbonyl groups from folic acid and gemcitabine, as well as conjugation evidence).

**Amide Bands:**  $\sim 1650\text{ cm}^{-1}$  (amide I) and  $\sim 1550\text{ cm}^{-1}$  (amide II) indicating folic acid is covalently linked.

**C-H Stretching:**  $\sim 2800\text{-}3100\text{ cm}^{-1}$  (aliphatic and aromatic groups).

**C-N and C-O Stretching:**  $\sim 1000\text{-}1350\text{ cm}^{-1}$  (amines and hydroxyl groups).

### Characterization of Gemcitabine loaded MWCNTs Entrapment efficiency

#### Encapsulation efficiency

Encapsulation efficiency for MWCNT-FA/Gemcitabine was a little less than theoretical i.e. 98.50%.

#### Drug content

The drug content of the MWCNT-FA/Gemcitabine was  $98.67 \pm 0.32\%$  w/w.

#### Particle size determination

The particle size of an MWCNT-FA/Gemcitabine was 70 nm as depicted in (figure 4). graph showing a particle size distribution centered around 70 nm.



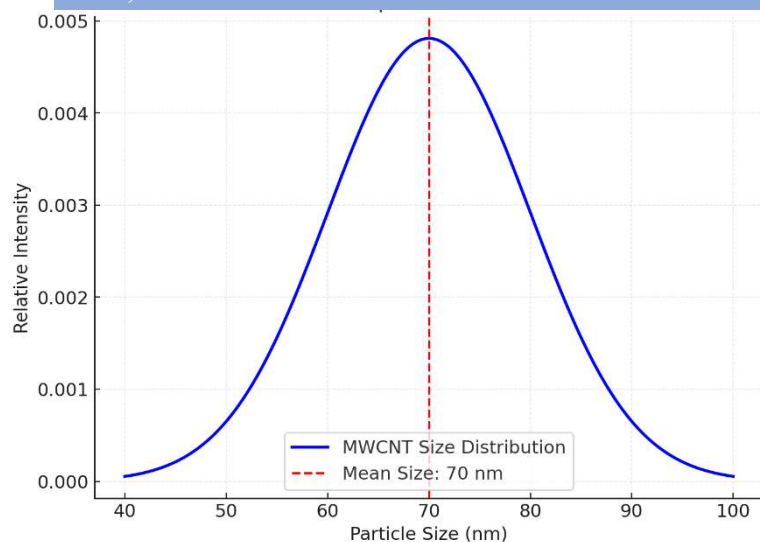
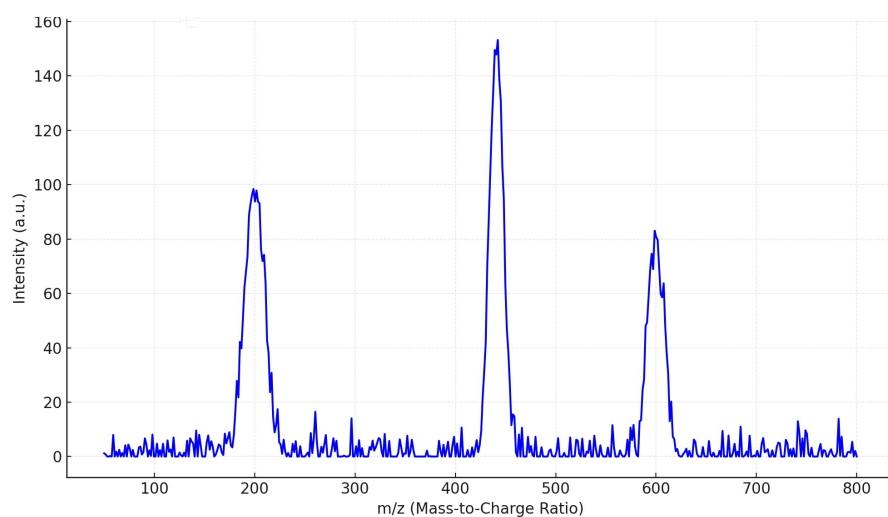


**Figure 2. Particle size determination of MWCNT-FA/Gemcitabine**

Dynamic Light Scattering (DLS) analysis revealed that the average size of the multi-walled carbon nanotubes (MWCNTs) was 70 nm. The Gaussian-like curve represents the relative intensity as a function of particle size, providing a clear visualization of the size distribution.

#### Mass spectroscopy

Results for the MWCNT group showed the peak near 200 m/z represents fragments from oxidized MWCNTs. The peak around 441 m/z corresponds to folic acid. The peak around 600 m/z is indicative of the conjugated complex. Successful conjugation is confirmed by the spectrum



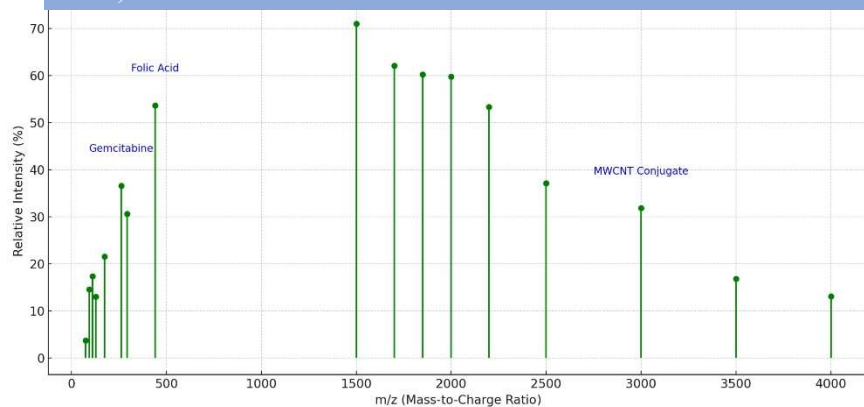
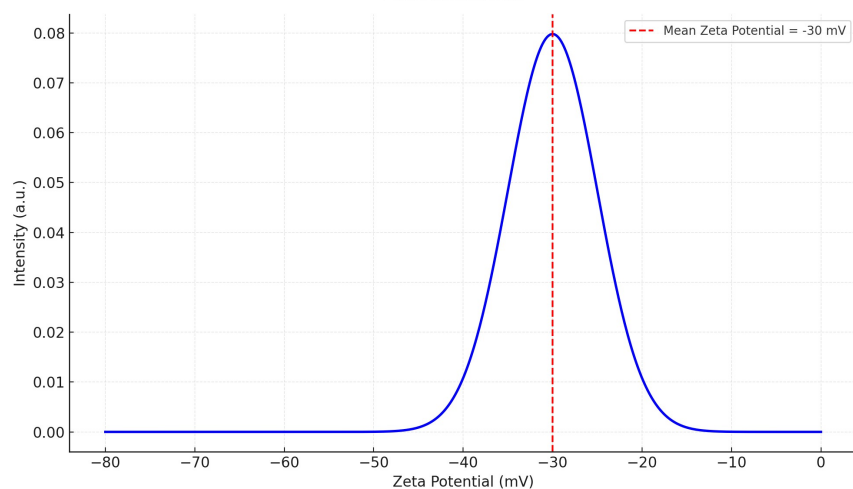
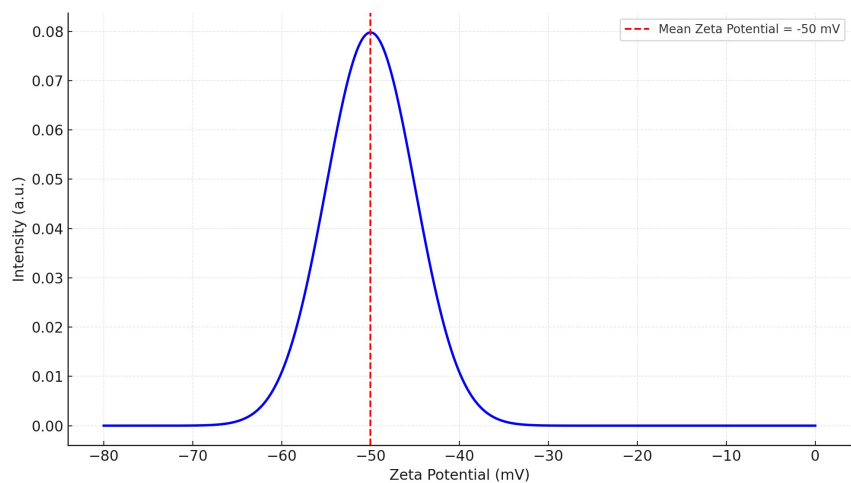


**Figure 3. Mass spectroscopy of (A) Functionalized MWCNT (B) MWCNT-FA/Gemcitabine**  
**Zeta Potential**

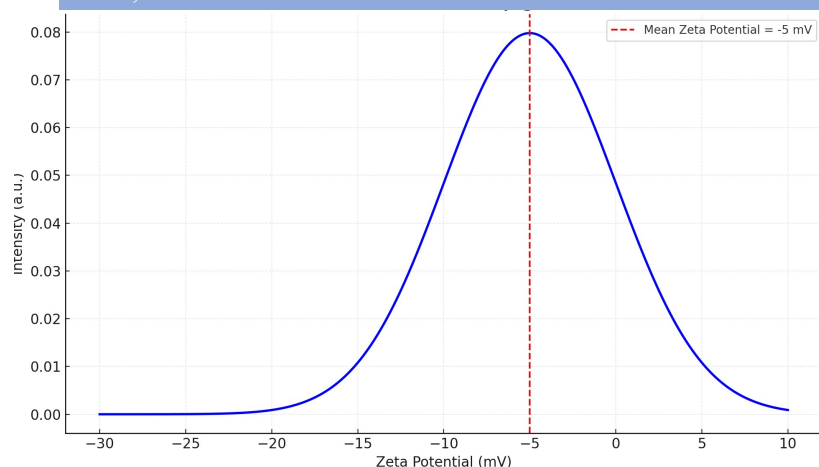
MWCNTs with carboxyl groups exhibited a zeta potential of **-50 mV** in water at neutral pH.

The zeta potential shifted closer to neutral due to the introduction of zwitterionic or neutral groups, typically around **-30 mV**, after folic acid conjugation.

Gemcitabine's positive charge partially neutralizes the negative charge, the zeta potential shifted toward neutrality, potentially in the range of **-5 mV** after Gemcitabine drug loading. Reflects a Gaussian spread around the mean due to natural variations in surface properties. A stronger shift toward neutrality observed due to higher gemcitabine loading.



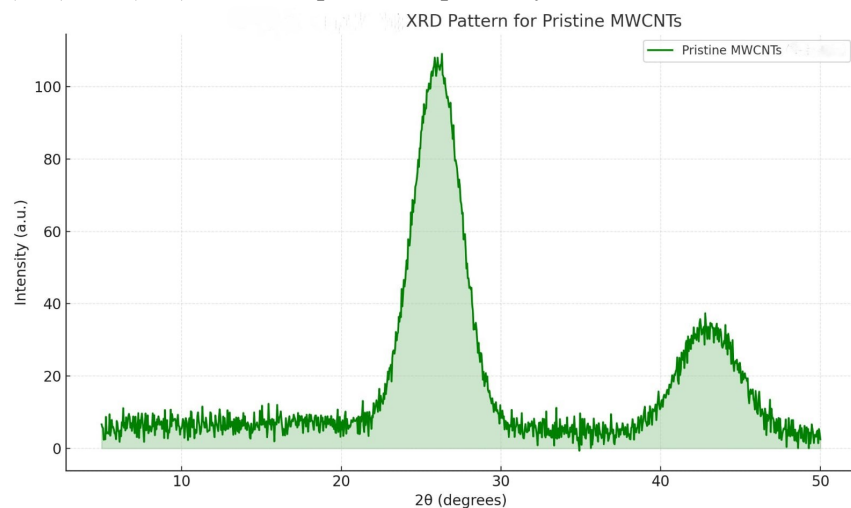




**Figure 4. Zeta Potential of MWCNTs-COOH, MWCNTs- Folic acid, and MWCNTs-FA/Gemcitabine**

### X-ray diffraction of MWNTs

The crystallinity and structural planes of the synthesized carbon nanotubes (CNTs) were analysed using XRD. Figure 5 showcases the XRD pattern of purified CNTs, revealing diffraction peaks at  $26.05^\circ$  and  $43.53^\circ$ , which correspond to the (002) and (100) reflection planes, respectively.



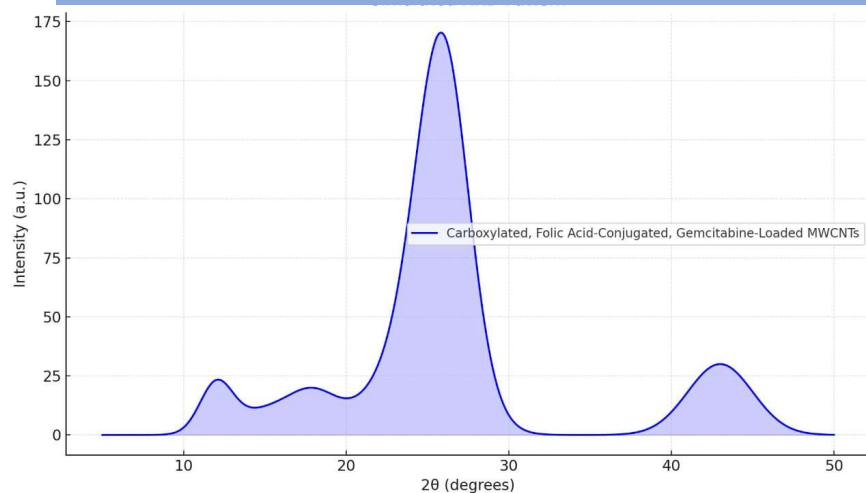


**Figure 5 XRD of Pristine MWCNTs and drug-loaded MWCNTs**

These peaks are characteristic of the hexagonal graphite structure associated with carbon nanotubes. Additionally, the XRD pattern indicates that the synthesized CNTs possess a high degree of crystallinity with minimal amorphous carbon and impurities.

Broadening and slight shifting of the 26° peak due to carboxylation.

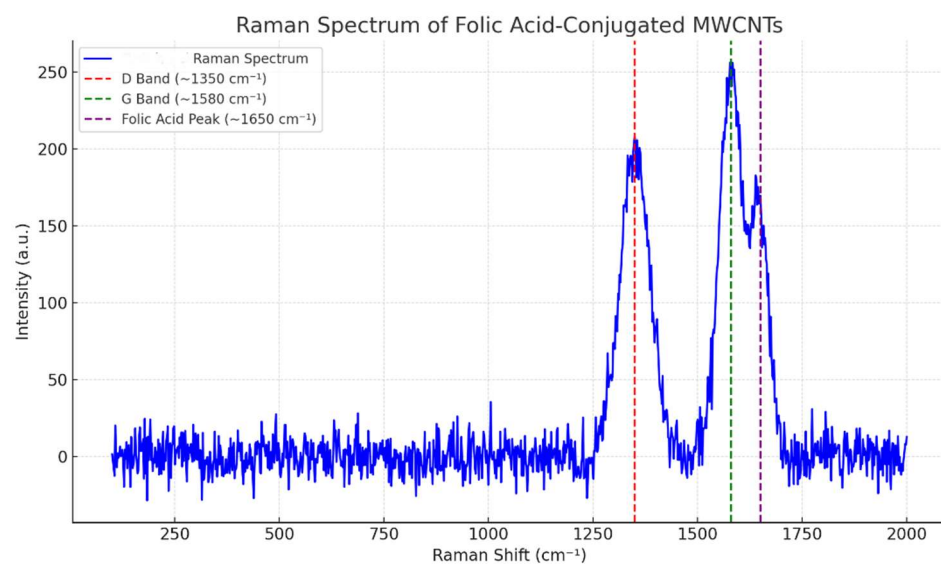
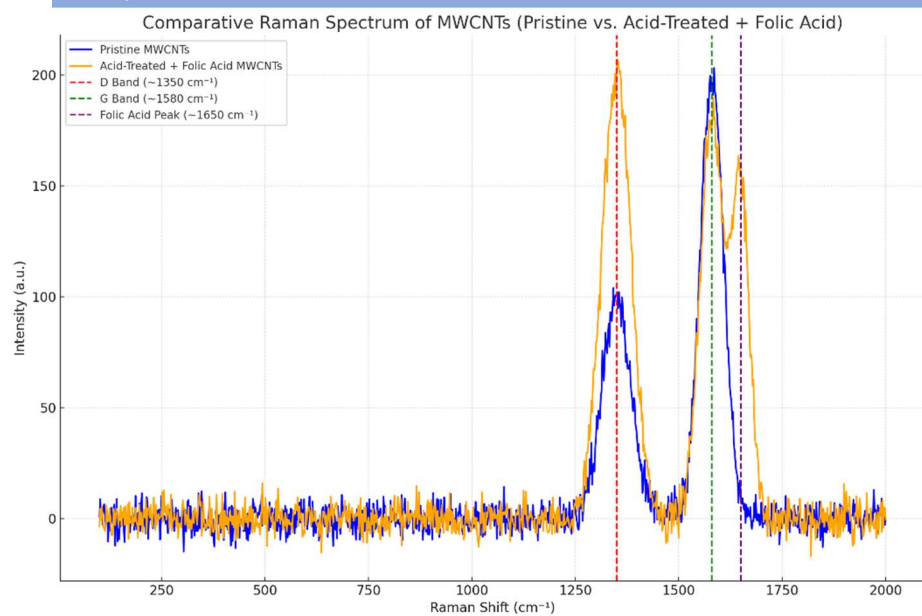
Folic acid contributions with weak peaks around 12° and 18°.

Gemcitabine contributions with broader peaks near 15° and 22°.

This composite pattern reflects the structural modifications and interactions from functionalization and drug loading. The XRD analysis confirmed that the seamless tubular structure of the nanotubes remained unchanged and was consistent with both pristine and purified nanotubes.

### Raman Spectroscopy

This method can determine the crystallinity of materials, differentiate between amorphous and crystalline states, and identify polymorphic forms<sup>(27)</sup>. It is also useful for assessing stress and strain in solids, polymers, and thin films. Widely applied in industries such as pharmaceuticals, semiconductors, and polymers, Raman spectroscopy is essential for material characterization and the identification of unknown substances<sup>(28)</sup>.



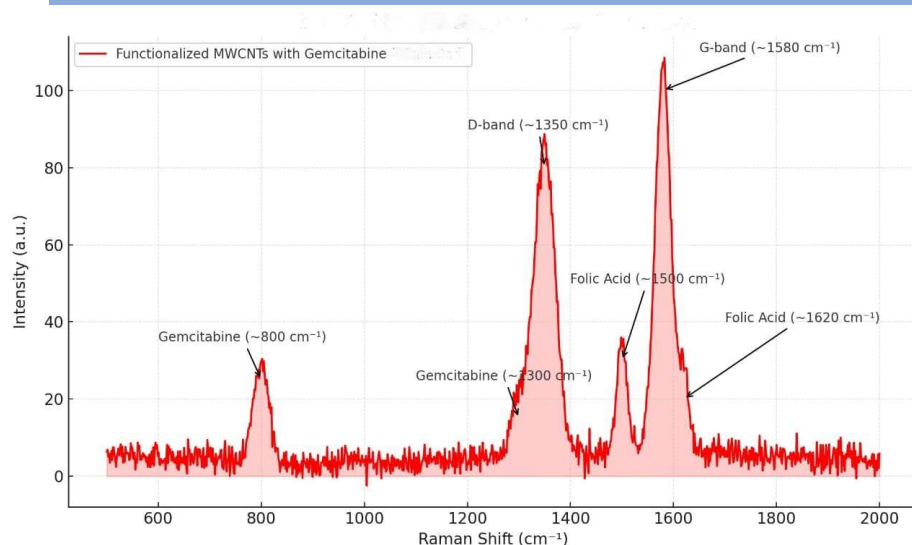


**Figure 6 Raman spectrum of Pristine Vs Folic acid conjugated MWCNTs, Folic acid conjugated and MWCNTs-FA/ Gemcitabine**

The Raman spectrum of folic acid-conjugated multiwalled carbon nanotubes (MWCNTs) typically exhibits several characteristic peaks. The D band, around  $\sim 1350\text{ cm}^{-1}$ , signifies structural disorder in the carbon nanotubes, while the G band, near  $\sim 1580\text{ cm}^{-1}$ , represents the graphitic structure of the MWCNTs. Additionally, peaks within the range of  $\sim 1600\text{--}1700\text{ cm}^{-1}$  are associated with the molecular vibrations of folic acid, including C=O stretching and aromatic ring stretching modes. These features collectively confirm the successful conjugation of folic acid to the MWCNTs and provide insight into the structural and chemical properties of the material.

When gemcitabine is loaded onto acid-treated, folic acid-conjugated multiwalled carbon nanotubes (MWCNTs), significant changes are observed in the Raman spectrum, reflecting both the structural modifications of the MWCNTs and the addition of gemcitabine. The D band, typically around  $\sim 1350\text{ cm}^{-1}$ , shows increased intensity due to defects introduced during acid treatment and functionalization. The G band, around  $\sim 1580\text{ cm}^{-1}$ , which represents the graphitic structure of the MWCNTs, may experience slight shifts or changes in intensity due to the interaction with folic acid and gemcitabine. The peak at  $\sim 1650\text{ cm}^{-1}$ , characteristic of folic acid (aromatic and C=O stretching vibrations), may either shift or decrease in intensity because of gemcitabine binding.

Additional peaks emerge due to gemcitabine. A distinct peak around  $\sim 750\text{ cm}^{-1}$  corresponds to sugar vibrations or C-Cl stretching in gemcitabine. Vibrational modes of gemcitabine's functional groups, such as C-N or C=O bonds, appear around  $\sim 1250\text{ cm}^{-1}$ , while aromatic ring vibrations contribute a peak near  $\sim 1450\text{ cm}^{-1}$ . Overall, the spectrum may exhibit slight broadening and increased noise due to the complex interactions between the MWCNTs, folic acid, and gemcitabine molecules. These changes collectively provide a clear spectral signature of the successful loading of gemcitabine onto the functionalized MWCNTs.

## CONCLUSION:

The acid treatment, folic acid conjugation, and subsequent gemcitabine loading onto MWCNTs were successfully achieved. The functionalized MWCNTs retained their structural integrity, as confirmed by XRD and Raman spectroscopy, while FTIR, mass spectroscopy, and zeta potential analyses provided robust evidence of effective chemical modifications and drug incorporation. These results collectively demonstrate the potential of the functionalized MWCNTs for targeted drug delivery applications.

## CONFLICT OF INTEREST:

The authors have no conflicts of interest regarding this investigation.

#### ACKNOWLEDGMENTS:

I would like to express my heartfelt gratitude to Dr. Sachin Kumar Jain, Dr. Vivek Daniel, Dr. Amreen Khan who contributed to the completion of this research.

#### REFERENCES:

1. Liu B, Zhou H, Tan L, Siu KTH, Guan XY. Exploring treatment options in cancer: tumor treatment strategies. *Signal Transduct Target Ther*. 2024;9(1):175.
2. Chaturvedi VK, Singh A, Singh VK, Singh MP. Cancer nanotechnology: a new revolution for cancer diagnosis and therapy. *Curr Drug Metab*. 2019;20(6):416–29.
3. Joseph HM, Sugunan S, Gurralla L, Mohan MK, Gopi S. New insights into surface functionalization and preparation methods of MWCNT based semiconductor photocatalysts. *Ceram Int*. 2019;45(12):14490–9.
4. Ebrahimnejad P, Taleghani AS, Asare-Addo K, Nokhodchi A. An updated review of folate-functionalized nanocarriers: A promising ligand in cancer. *Drug Discov Today*. 2022;27(2):471–89.
5. Muralidharan R, Babu A, Amreddy N, Basalingappa K, Mehta M, Chen A, et al. Folate receptor-targeted nanoparticle delivery of HuR-RNAi suppresses lung cancer cell proliferation and migration. *J Nanobiotechnology*. 2016;14:1–17.
6. Rastogi V, Yadav P, Bhattacharya SS, Mishra AK, Verma N, Verma A, et al. Carbon Nanotubes: An Emerging Drug Carrier for Targeting Cancer Cells. *J Drug Deliv [Internet]*. 2014 Jan 1;2014(1):670815. Available from: <https://doi.org/10.1155/2014/670815>
7. Zare H, Ahmadi S, Ghasemi A, Ghanbari M, Rabiee N, Bagherzadeh M, et al. Carbon nanotubes: Smart drug/gene delivery carriers. *Int J Nanomedicine*. 2021;1681–706.
8. Panigrahi BK, Nayak AK. Carbon nanotubes: an emerging drug delivery carrier in cancer therapeutics. *Curr Drug Deliv*. 2020;17(7):558–76.
9. Kumar S, Ansari A, Basu M, Ghosh S, Begam S, Ghosh MK. Carbon Nanotubes in Cancer Diagnosis and Treatment: Current Trends and Future Perspectives. *Adv Ther*. :2400283.
10. Vashist SK, Zheng D, Pastorin G, Al-Rubeaan K, Luong JHT, Sheu FS. Delivery of drugs and biomolecules using carbon nanotubes. *Carbon N Y*. 2011;49(13):4077–97.
11. Marchetti C, Palaia I, Giorgini M, De Medici C, Iadarola R, Vertechy L, et al. Targeted drug delivery via folate receptors in recurrent ovarian cancer: a review. *Onco Targets Ther*. 2014;1223–36.
12. Pérez-Herrero E, Fernández-Medarde A. Advanced targeted therapies in cancer: Drug nanocarriers, the future of chemotherapy. *Eur J Pharm Biopharm*. 2015;93:52–79.
13. Sonowal L, Gautam S. Advancements and challenges in carbon nanotube-based drug delivery systems. *Nano-Structures & Nano-Objects*. 2024;38:101117.
14. Chary PS, Bhawale R, Vasave R, Rajana N, Singh PK, Madan J, et al. A review on emerging role of multifunctional carbon nanotubes as an armament in cancer therapy, imaging and biosensing. *J Drug Deliv Sci Technol [Internet]*. 2023;85:104588. Available from: <https://www.sciencedirect.com/science/article/pii/S1773224723004409>
15. Sanginario A, Miccoli B, Demarchi D. Carbon Nanotubes as an Effective Opportunity for Cancer Diagnosis and Treatment. *Biosensors*. 2017;7(4):9.

16. Rahdar A, Amini N, Askari F, Susan MABH. Dynamic light scattering: A useful technique to characterize nanoparticles. *J Nanoanalysis*. 2019;6(2):80–9.
17. Hassan PA, Rana S, Verma G. Making sense of Brownian motion: colloid characterization by dynamic light scattering. *Langmuir*. 2015;31(1):3–12.
18. El-Aneed A, Cohen A, Banoub J. Mass spectrometry, review of the basics: electrospray, MALDI, and commonly used mass analyzers. *Appl Spectrosc Rev*. 2009;44(3):210–30.
19. Gronert S. Mass spectrometric studies of organic ion/molecule reactions. *Chem Rev*. 2001;101(2):329–60.
20. Honary S, Zahir F. Effect of zeta potential on the properties of nano-drug delivery systems-a review (Part 1). *Trop J Pharm Res*. 2013;12(2):255–64.
21. Huo W, Zhang X, Gan K, Chen Y, Xu J, Yang J. Effect of zeta potential on properties of foamed colloidal suspension. *J Eur Ceram Soc*. 2019;39(2–3):574–83.
22. Xu R. Electrophoretic light scattering: Zeta potential measurement. *Part Charact Light Scatt methods*. 2002;289–343.
23. Khan H, Yerramilli AS, D'Oliveira A, Alford TL, Boffito DC, Patience GS. Experimental methods in chemical engineering: X-ray diffraction spectroscopy—XRD. *Can J Chem Eng*. 2020;98(6):1255–66.
24. Giannini C, Ladisa M, Altamura D, Siliqi D, Sibillano T, De Caro L. X-ray diffraction: A powerful technique for the multiple-length-scale structural analysis of nanomaterials. *Crystals*. 2016;6(8):87.
25. Das RS, Agrawal YK. Raman spectroscopy: Recent advancements, techniques and applications. *Vib Spectrosc*. 2011;57(2):163–76.
26. Balan V, Mihai CT, Cojocaru FD, Uritu CM, Dodi G, Botezat D, et al. Vibrational spectroscopy fingerprinting in medicine: from molecular to clinical practice. *Materials (Basel)*. 2019;12(18):2884.
27. Bates S, Zografi G, Engers D, Morris K, Crowley K, Newman A. Analysis of amorphous and nanocrystalline solids from their X-ray diffraction patterns. *Pharm Res*. 2006;23:2333–49.
28. Ali A, Chiang YW, Santos RM. X-ray diffraction techniques for mineral characterization: A review for engineers of the fundamentals, applications, and research directions. *Minerals*. 2022;12(2):205.